

SBIR Phase I Final Report

29 January, 2010 - 29 July, 2010

Submitted by: Jacqueline H. Hines (PI)
 Phone: 410-544-4664; Fax: 410-544-4665; jhines@asrdcorp.com
 July 29, 2010

1. Quantitative description of work performed during this period

ASR&D completed the phase I program effort during this reporting period.

Task 4.1.1 & 8 – Program Management: ASR&D completed and submitted this final report, and a proposal for continued sensor development work under a Phase 2 program.

Task 4.1.2 – Gas Dilution Test Setup Development:

An electrical sensor test fixture with a Teflon vapor-tight cap developed was reported previously. During this project, all vapor testing was performed using this fixture and an Environics 4040 vapor generator was for calibrated gas dilution and flow control. A schematic of the system is shown below.

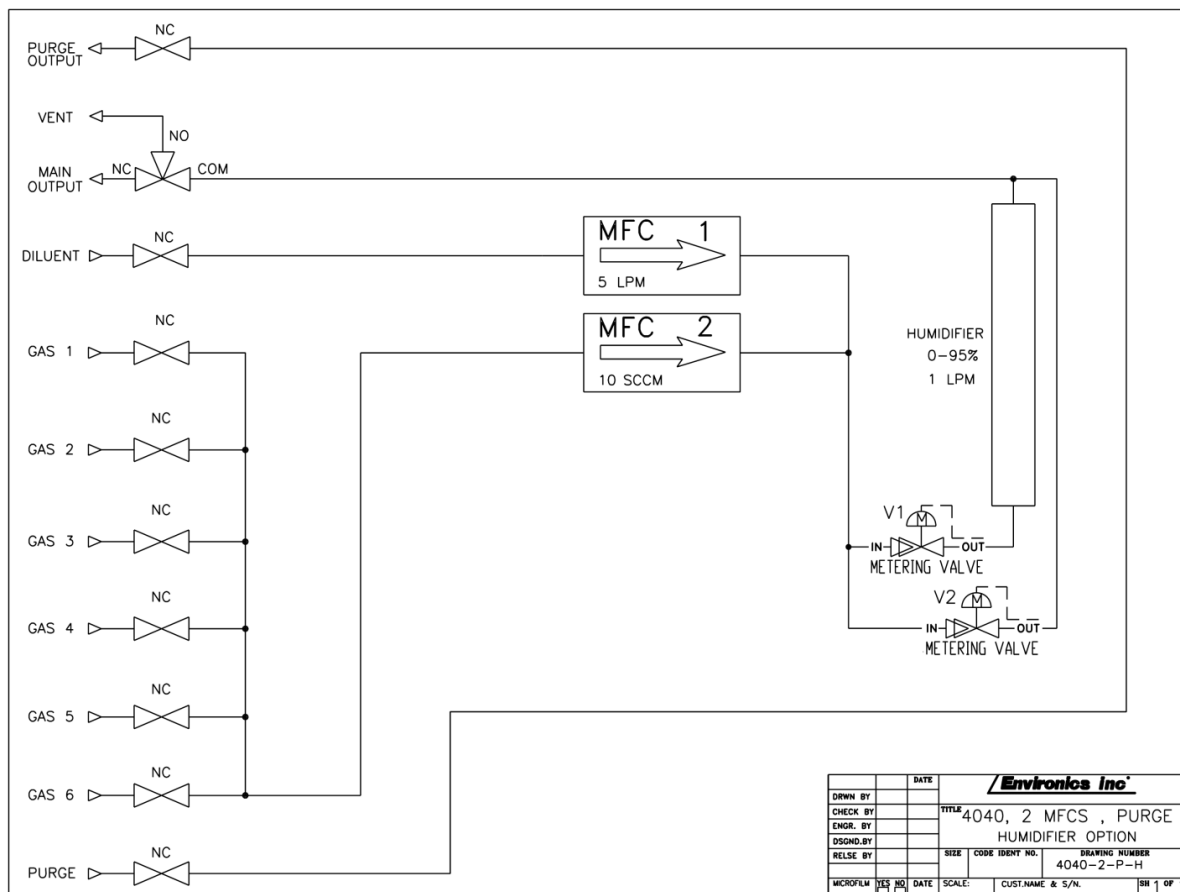


Figure 1. Schematic of Environics 4040 gas dilution system. All of the ports are solenoid controlled valves.

Table 1. Gas connection table

Port Name	Gas connected and pressure
Diluent	N ₂ @ 25 psi
Gas 1	0.1% H ₂ in N ₂ @25 psi
Gas 2	1% CH ₄ in N ₂ @25 psi
Gas 3	8% H ₂ in N ₂ @25 psi
Gas 5	None Connected
Gas 6	None Connected
Purge	N ₂ @ 25 psi

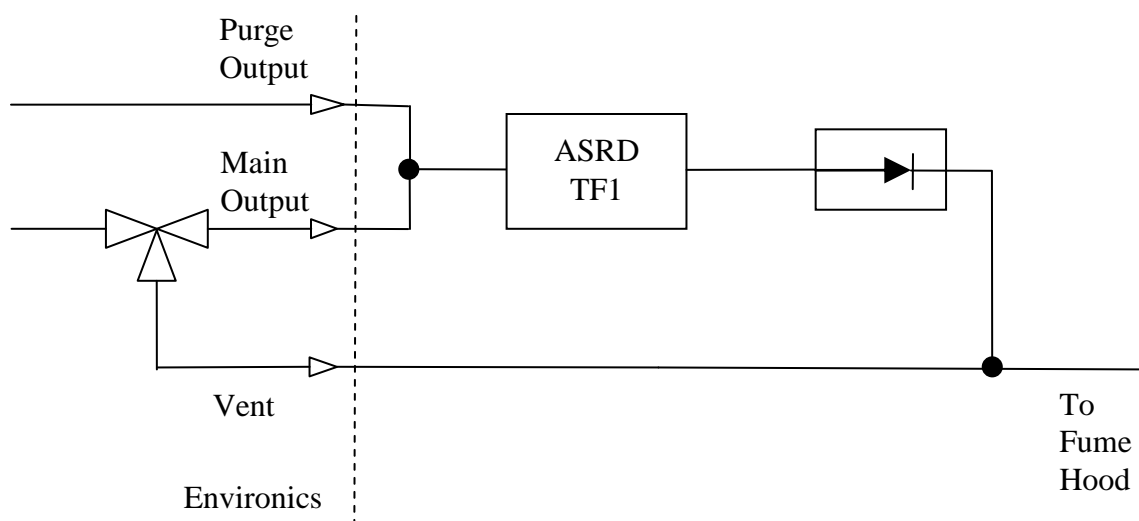


Figure 2. Schematic of gas routing from Environics to the test fixture, ASRD TF1.

One limitation of the Environics gas dilution system that was unanticipated is that it can take from 20-30 seconds up to 4 minutes to establish a stable concentration of gas to use in sensor testing. For example, to flow 1 ppm H₂ using the 0.1% H₂ tank flowing at 1 LPM, it takes 4 minutes for MFC2 to start flowing gas at the correct rate to produce the desired concentration. This presented a problem when testing devices that potentially respond in less than a second, as what appears to be a delay in sensor response may actually be a real-time measurement of the gas concentration ramping up within the Environics system.

The engineering team at Environics was contacted to try and find a solution for this problem. They were able to suggest a change in the settings of the software that controlled the system that would allow for different combinations of solenoid valve activations. This made it possible to choose when mixed gas would flow to the vent or flow to the main output (and over the sensor). The system was configured such that the solenoid valves could be activated to allow either purge gas or mixed gas to flow out the main output. It also made it possible to

activate the purge line while gas was flowing to the vent line, and therefore maintain gas flow over the device.

ASRD then began testing devices using a setup where the mixed gas was diverted to the vent line for a period of time sufficient to allow mixing to concentration, with purge gas (N₂) flowing over the sample under test. Purge gas in this configuration flows at an uncontrolled rate, based solely on the pressure in the nitrogen supply line (typically about 40-60 psig). The result of that test is shown in Figure 3 below.

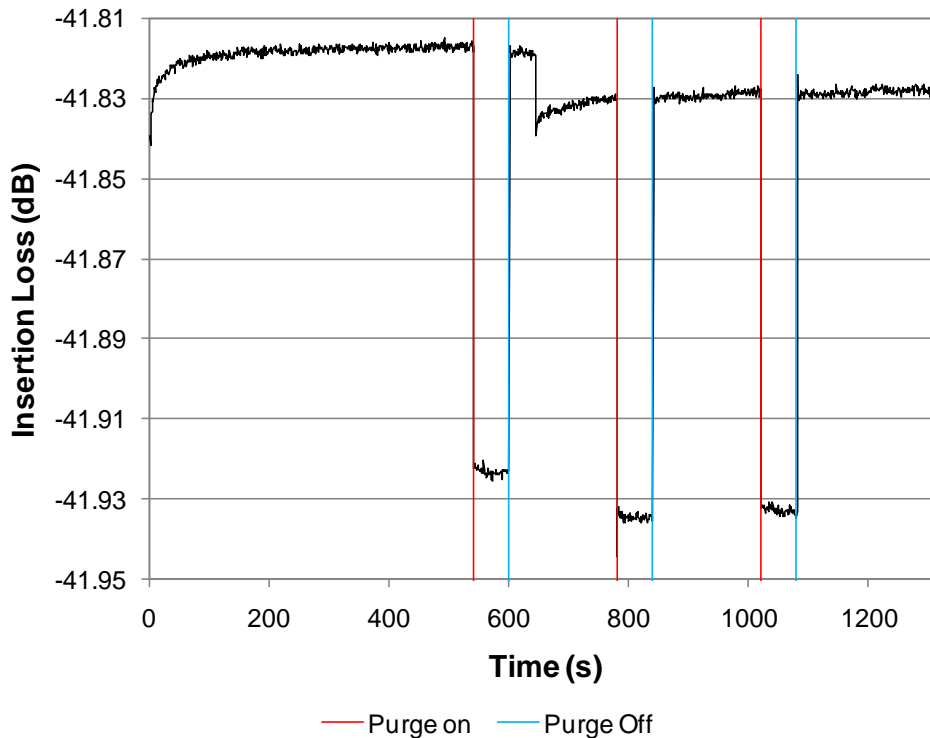


Figure 3. Testing of a cryptophane coated device with cycling CH₄ using a the purge line to flow gas while the mixed gas is going to vent.

In Figure 3 only the purge on and off times are highlighted. The sensor response to the methane is overwhelmed by the response of the sensor to the flow rate variations between controlled flow at 1 lpm from the Environics (during purge off period) and nitrogen being flowed in an uncontrolled fashion from the purge line. This was not an acceptable method for testing.

During the next test the purge valves remained closed throughout the testing to avoid the radical changes in flow observed above. Instead, to provide enough time to allow the sample gas and diluent to mix to the appropriate concentration without exposing the sensor to gas of changing concentration, the mixed gas was diverted to vent, and no gas was flowing over the sensor during the mixing time. Once the correct concentration was reached, flow was redirected over the

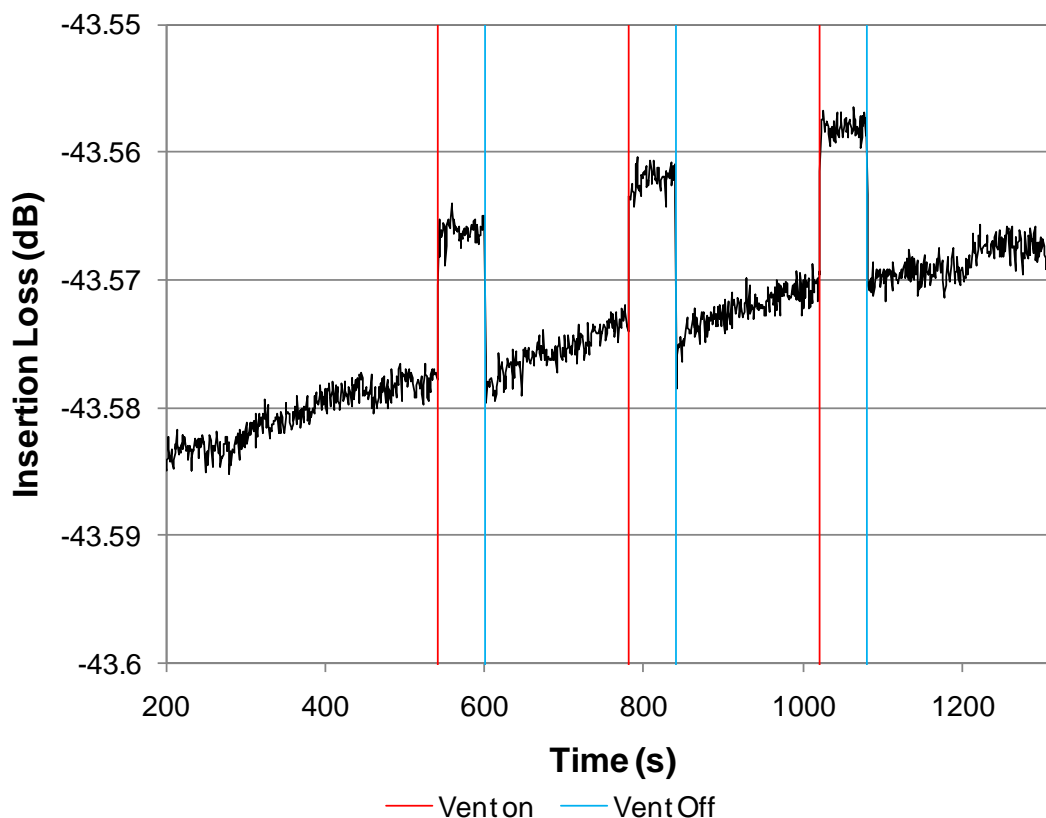


Figure 4. Response of an OTMS coated die (no vapor sensitive film) to the gas flow being diverted to the vent line and stopping gas flow over the die.

sensor. As shown in Figure 4, an unacceptably large change in sensor response was seen for time periods where the vapor was diverted to vent (with no flow over the sensor) as compared to periods of flow over the sensor. These results were observed using a sensor coated only with octadecyltrimethoxysilane (OTMS), a film that is not chemically sensitive to either hydrogen or methane, in order to separate the effects of flow from possible film/vapor interactions.

What was needed was a method to control the flow of gas in the purge line to match the flow rate coming out of the Environics system. Then the sensor would not see any change in flow when switching between the gas being vented (for mixing) and flowing over the sensor, eliminating transients due to gas flow rates.

A Swagelok low-flow metering valve was purchased and installed in the gas line feeding the purge port. After installing this valve a SAW sensor was placed in the test fixture and gas was cycled between gas flowing from the output at 1 lpm and gas flowing from the purge line. By watching the change in the response of the sensor to switching between the controlled flow coming from MFC1 and from the purge line, the metering valve was adjusted to make the response the same for the two flows. This fixed the flow variation problem, and this system configuration was used in the remainder of the testing shown in this report.

The concentration of the gas canisters used in conjunction with the EnviroNics system determined what gas concentrations and flow rates could be achieved. The following table gives the maximum and minimum gas concentrations that can be generated for a given canister concentration.

Initial Concentration (%)	Maximum Concentration with both flow meters (ppm)	Minimum Concentration with both flow meters (ppm)	Gas
0.1	19.6	0.200	H ₂
1	196.1	2.000	CH ₄
8	1568.6	15.997	H ₂

Table 2. Maximum and minimum gas concentrations achievable with the EnviroNics for a given initial source gas concentration.

At a given canister concentration only a certain range of gas concentrations and flow rates were achievable given the mass flow controllers in the EnviroNics system. The table below gives the maximum and minimum gas flow rates for different sample gas concentrations for the different source gas canisters.

Final Concentration	Min Flow Rate	Max Flow Rate	Source Gas
1000 ppm	0.51 LPM	0.8 LPM	8 % H ₂
100 ppm	.8 LPM	5 LPM	8 % H ₂
10 ppm	0.5 LPM	1 LPM	0.1 % H ₂
1 ppm	1 LPM	5 LPM	0.1 % H ₂
196 ppm	0.51 LPM	0.51 LPM	1 % CH ₄
20 ppm	0.5 LPM	5 LPM	1 % CH ₄
2 ppm	5 LPM	5 LPM	1 % CH ₄

Table 3. Maximum and minimum gas flow rates for different gas dilutions.

If a higher concentration was required for testing a sensor, the gas manifold feeding the EnviroNics could be manually configured such that the source gas could flow into the diluent port of the EnviroNics. This was done with the CH₄ testing to expose the sample to 1% CH₄; and for initial responses of Pd films to H₂ it proved to be the most expedient way to age the Pd film.

Task 4.1.3 – Hydrogen Sensor Fabrication: During this project, ASR&D used reflective power spectral density (PSD) devices fabricated previously both as in-situ monitors for Pd deposition and as substrates for Pd deposition to form hydrogen sensors. Octadecyltrimethoxysilane (OTMS) was deposited on all of the devices prior to wafer dicing, solvent cleaning, and Pd deposition. Reflective delay line sensors were also used for comparison purposes. The Temescal e-beam system was used to deposit a thin layer of Pd onto several different in-situ monitor devices (during multiple different Pd deposition runs), and onto defined portions of several OTMS-coated PSD devices. The regions of the sensor devices onto which Pd was deposited were defined by Kapton tape for half of the devices, and by photoresist for the other half of the devices. Following Pd deposition, a standard acetone, methanol, isopropyl alcohol rinse was used for liftoff to remove the photoresist and Pd on top of the resist. The performance

and hydrogen response of devices fabricated with these two methods were evaluated, and the photolithographically defined Pd films had almost no response to hydrogen exposure. This was substantially worse than the hydrogen response of films defined by physical masking, and thus it was determined that standard photolithographic processes cannot be used to pattern e-beam deposited Pd for hydrogen sensor use. Alternate film definition techniques need further evaluation. Test results are shown under task 4.1.6 (sensor testing).

Task 4.1.4 – Methane Sensor Development: Dr. Douglas B. Hausner, working with the Borguet team at Temple University, successfully synthesized, purified, and characterized cryptophane-A (C_{3h}), a compound known to interact with methane. The synthesis technique used was the two-step process of Collet et al. [1], which is shown schematically in Figure 5. The synthesized compound was characterized with nuclear magnetic resonance (NMR). Initial attempts produced samples that were less pure than desired, as evidenced by the NMR spectra shown in Figure 6. A second synthesis was performed, resulting in isolation of significantly more pure cryptophane-A. The NMR spectrum for the cryptophane-A synthesized at Temple University is shown in Figure 7, where it is compared to the spectrum for cryptophane-E (from literature [2]). For 1H -NMR spectra, peaks

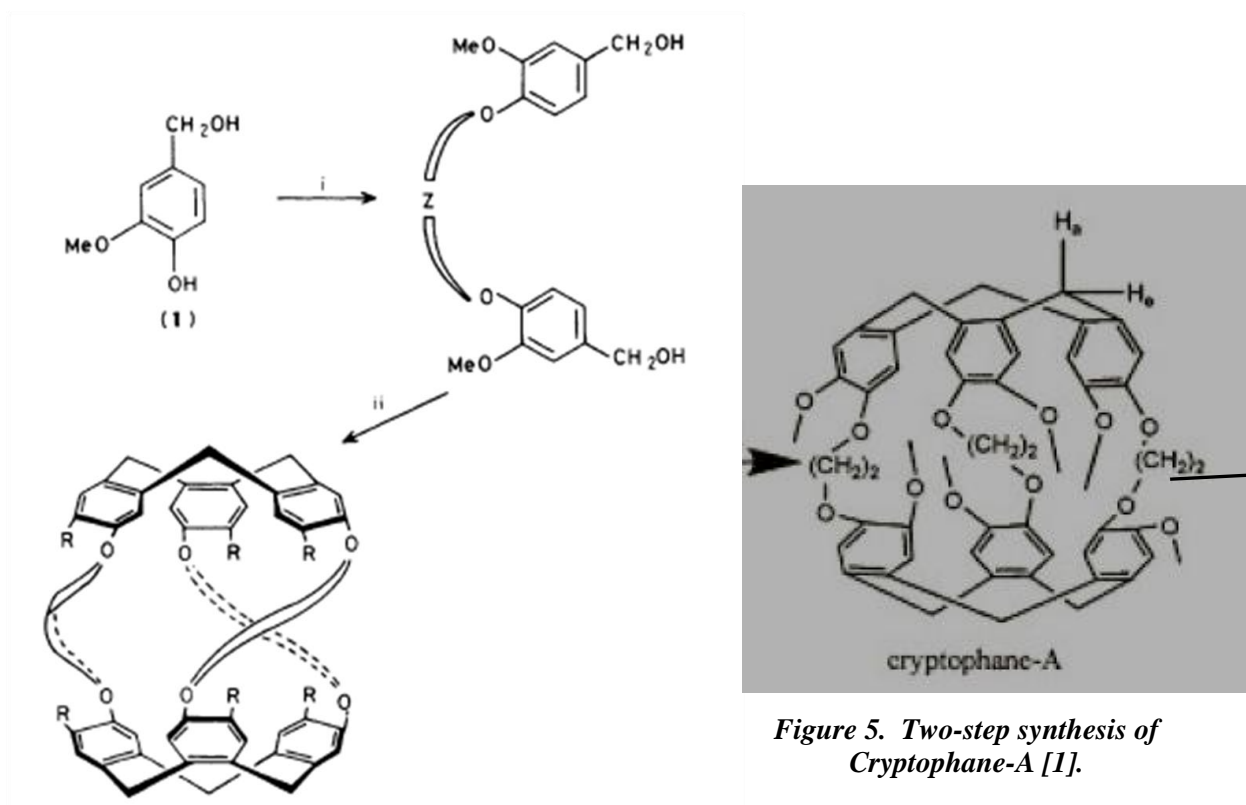


Figure 5. Two-step synthesis of Cryptophane-A [1].

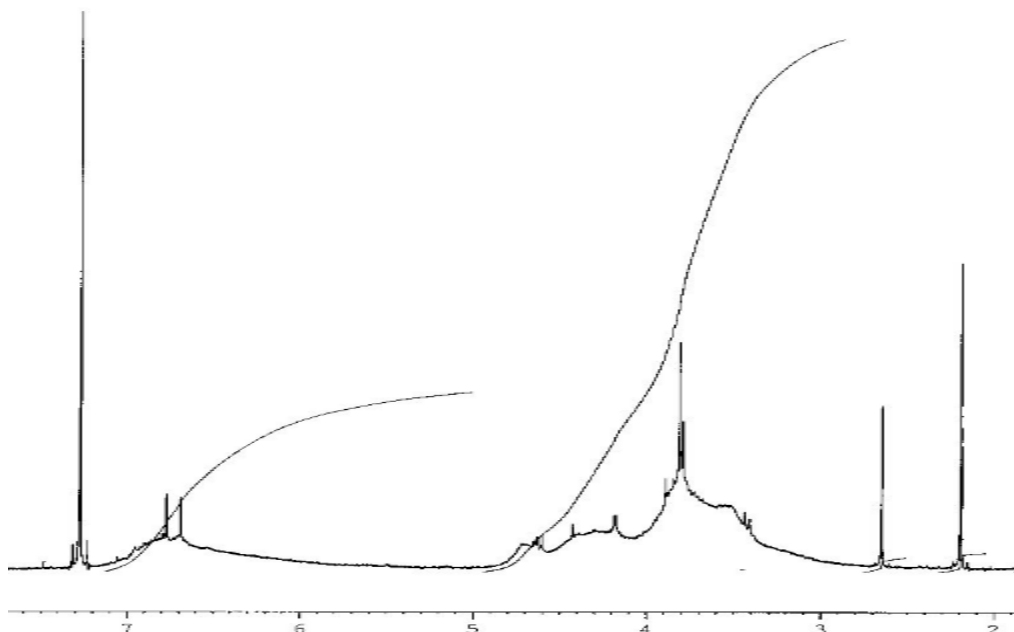


Figure 6. NMR spectra of first purification of cryptophane-A synthesized by Temple University team. Broad responses indicates need for further purification.

peaks at approximately 7 ppm correspond to aromatic protons, 4.5 ppm peaks correspond to bridging protons [O-(CH₂)₂-O], and 3.75 ppm peaks correspond to methoxy (-OCH₃) protons. The difference between cryptophanes A and E is the doublet peak at approximately 3.4 ppm (due to [O-(CH₂)₃-O] in cryptophane E), shown circled in Figure 7. This spectrum confirms that the team has isolated cryptophane-A.

The Temple team deposited initial cryptophane-A films on glass slides and evaluated the infrared (IR) spectra. Figure 8 shows a comparison of the IR spectrum taken at Temple and a reference spectrum from literature [3]. The Temple spectrum is cut off below 2000 cm⁻¹ due to lack of IR transmission through the glass substrate. Conventional FTIR of film samples on glass exposed to methane gas (CH₄) was unable to discern film/vapor interaction responses, due to transmission through the gas phase producing a gas phase signal that swamped the small interaction signal of interest. In order to overcome this problem, the Temple team utilized attenuated total reflectance (ATR) in conjunction with FTIR. ATR (Figure 5) is a method where the optical signal is effectively confined within a slide that provides nearly total internal reflection of the IR along the signal path. On one side of the slide, the sample layer (cryptophane-A) is deposited. The IR signal interacts with the sample, which modifies the optical reflection properties, each time it is reflected off of this side of the slide. In this manner, small changes in the IR beam due to interactions between a gas phase analyte and a layer can be measured, without the IR signal propagating through the gas phase. The ATR-FTIR spectra of the cryptophane-A films fabricated by Temple were taken with and without exposure of the film to CH₄. As can be seen in Figure 10, the change in the overall spectrum is due to

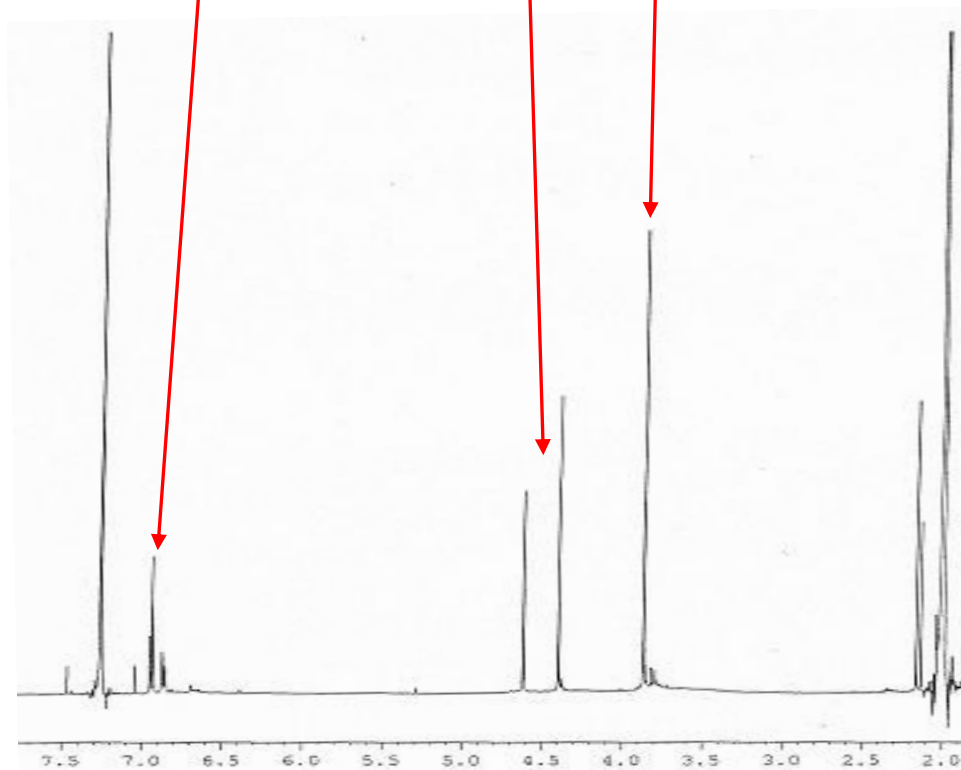
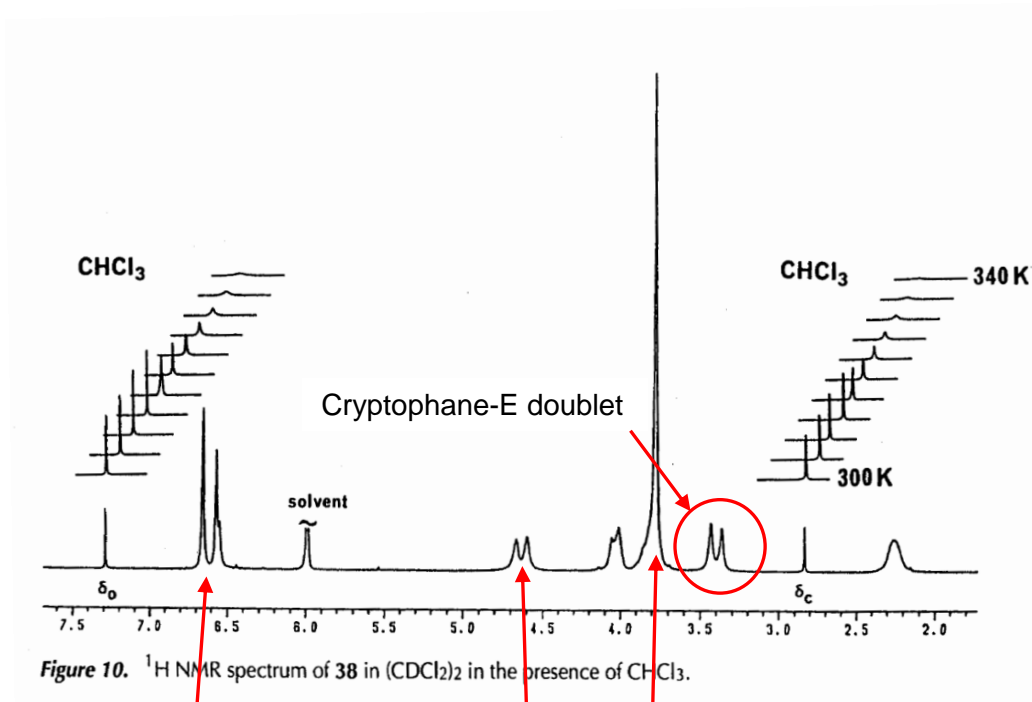


Figure 7. NMR spectra of second purification of cryptophane-A synthesized by Temple University team (bottom) compared to cryptophane-E reference spectrum.

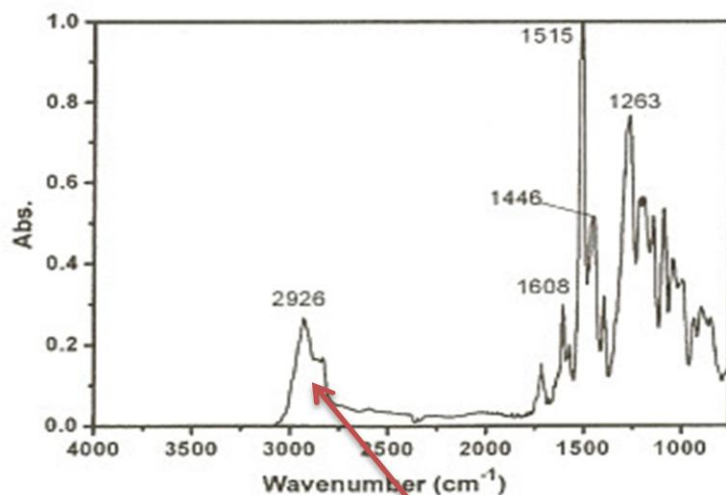


Fig. 3. The FTIR spectrum of the cryptophane-A.

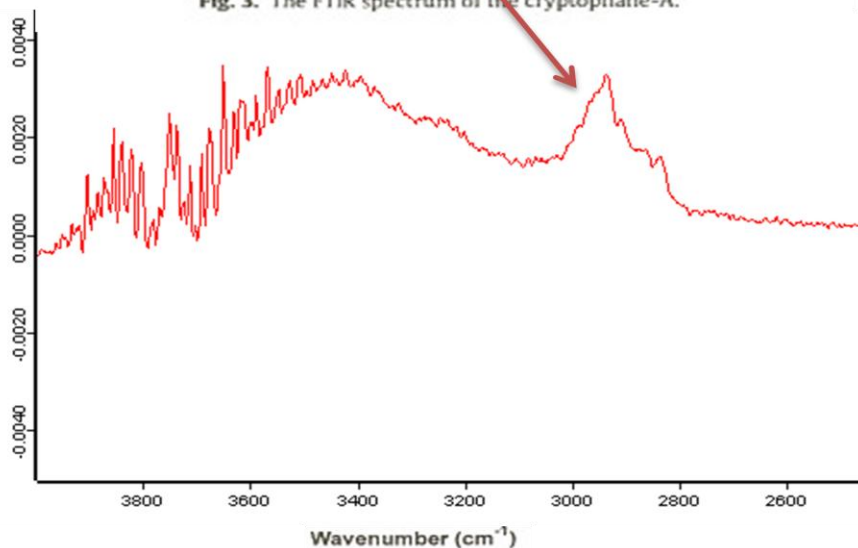


Figure 8. FTIR spectra of cryptophane-A synthesized by Temple University team (bottom) compared to cryptophane-A reference FTIR spectrum [3].

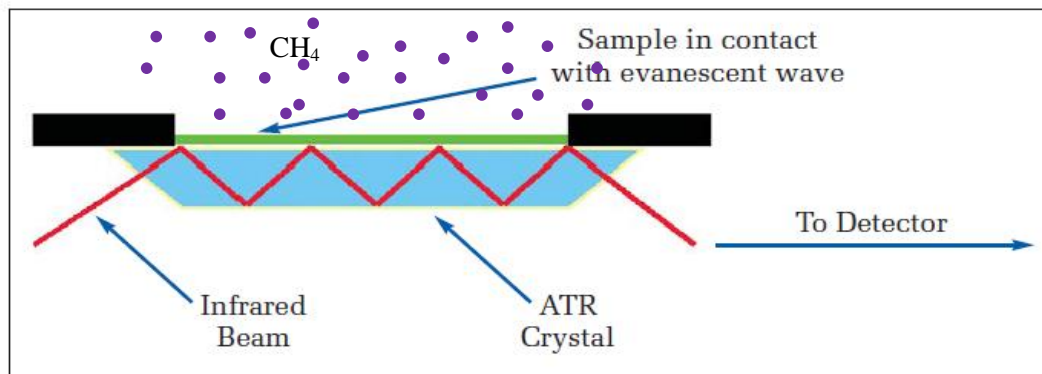


Figure 9. Attenuated total reflectance FTIR test setup. The green layer represents the cryptophane-A film deposited on top of the ATR slide.

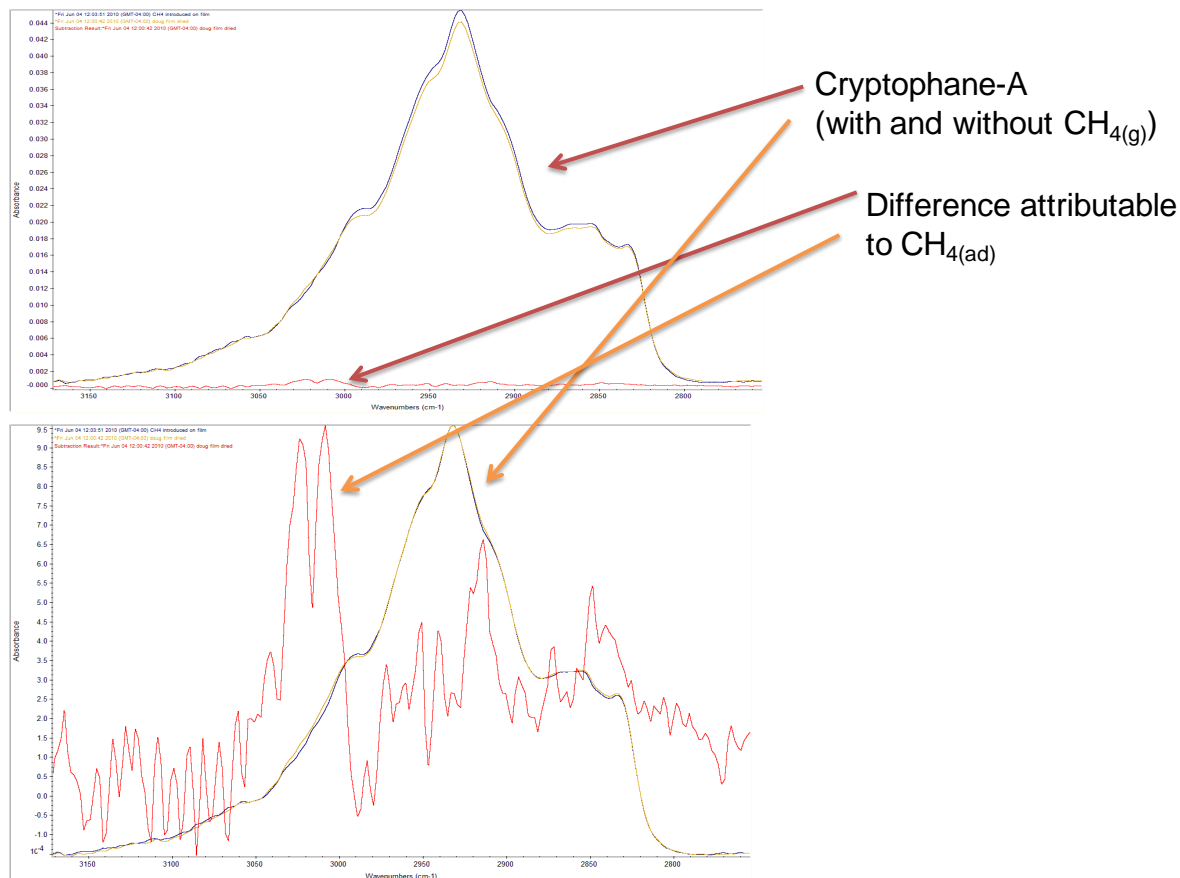


Figure 10. ATR-FTIR spectra of cryptophane-A with and without exposure to gas phase (g) CH_4 . The calculated difference spectrum, shown in red, is due to the interaction of the film with CH_4 .

CH_4 is quite small, and in order to make the effects more clear, a difference spectrum is calculated. The upper plot of Figure 10 shows the difference spectrum (in red) on the same scale as the overall spectrum. The scale of the difference spectrum has been modified in the lower plot of Figure 10, to show in greater detail the change produced by adsorbed $CH_{4(ad)}$. In order to make sure that the change in ATR-FTIR signal seen is due to an interaction between methane gas and the cryptophane film, difference spectra calculated from measurements made with and without the cryptophane-A film present are compared. Figure 11 shows these two spectra. The red spectrum is for gas phase CH_4 with no cryptophane-A film present. The blue spectrum is for the cryptophane-A film interacting with gas phase CH_4 , and the splitting seen is due to a change in symmetry of the CH_4 which is indicative of binding. These ATR-FTIR responses clearly demonstrate that methane is interacting with the cryptophane -A film. In order to determine if this interaction is measurable acoustically, these films were deposited onto SAW sensors at ASR&D. Measurements of methane response were quite weak, as shown in Figure 12. Additional research uncovered several possible film modifications and deposition techniques for cryptophane that are likely to significantly enhance the film sensitivity. These techniques have been included in a proposal for a Phase 2 continuation of this research.

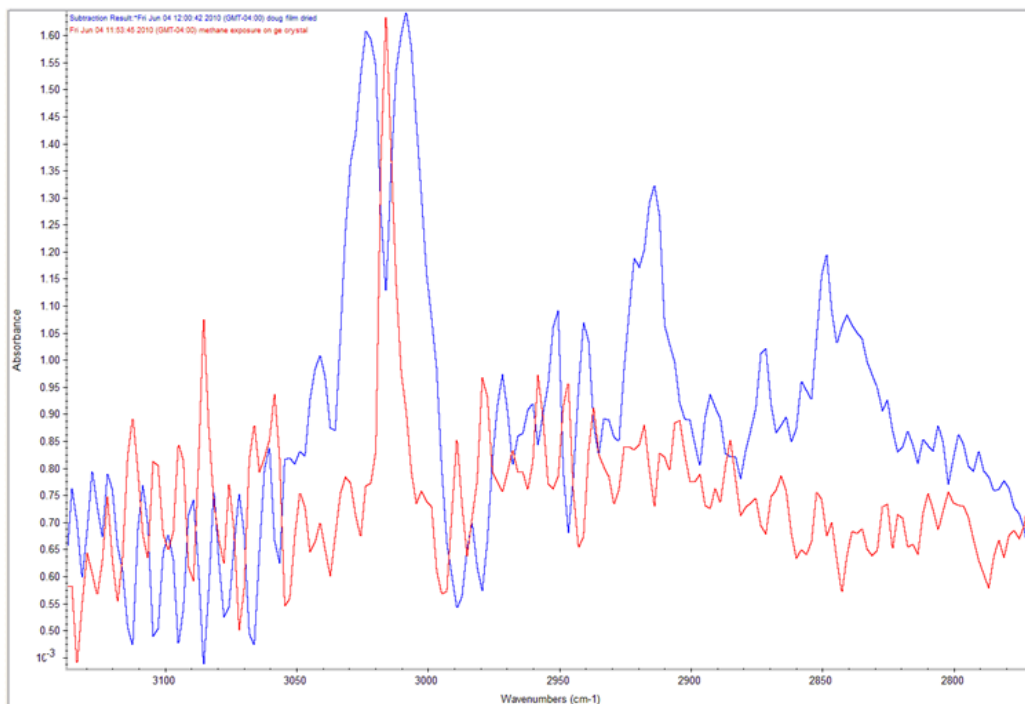


Figure 11. ATR-FTIR difference spectra of gas phase (g) CH_4 with (blue) and without (red) cryptophane-A film present. Splitting is characteristic of CH_4 interacting with the film.

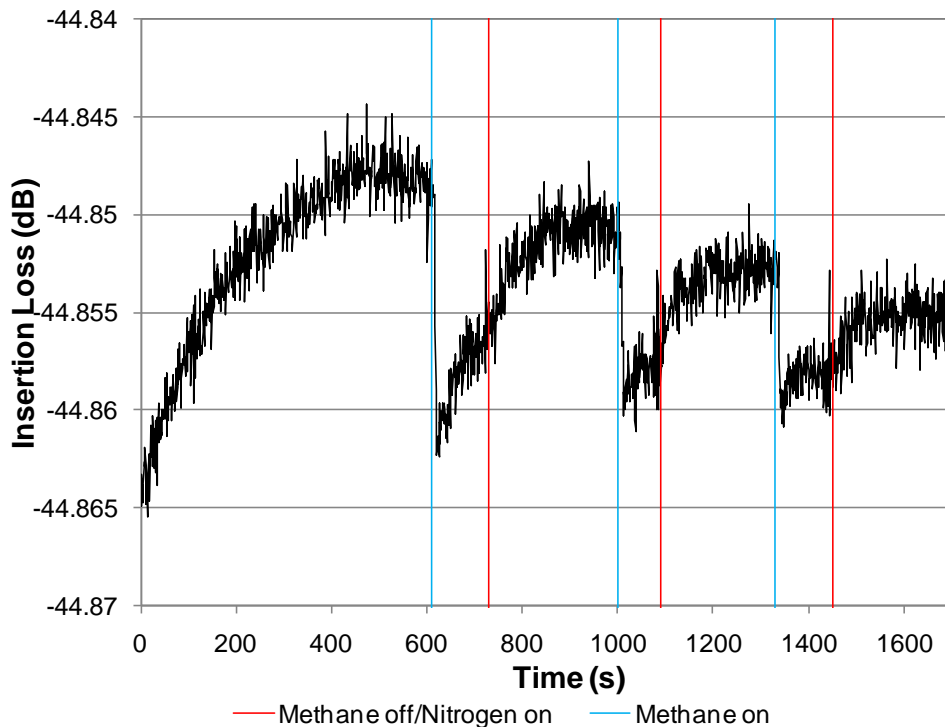


Figure 12. Response of sensor with spin-coated cryptophane-A film to 1% CH_4 with N_2 carrier gas.

indicates that the actual thickness of this film is about 34Å, not the 14Å indicated by the QCM monitor. The SAW deposition monitor provides a significantly better approach to determining film thickness for very thin conductive films. We also note that the Pd films have a clear nanocluster morphology. Figure 16 shows an AFM scan showing the morphology of film deposited by ASR&D. The bright dots in the right image correspond to the peaks shown in the three dimensional rendering on the left. These features have sizes ranging from tens of nm up to about 150nm, and appear to correspond to clustering of the Pd film.

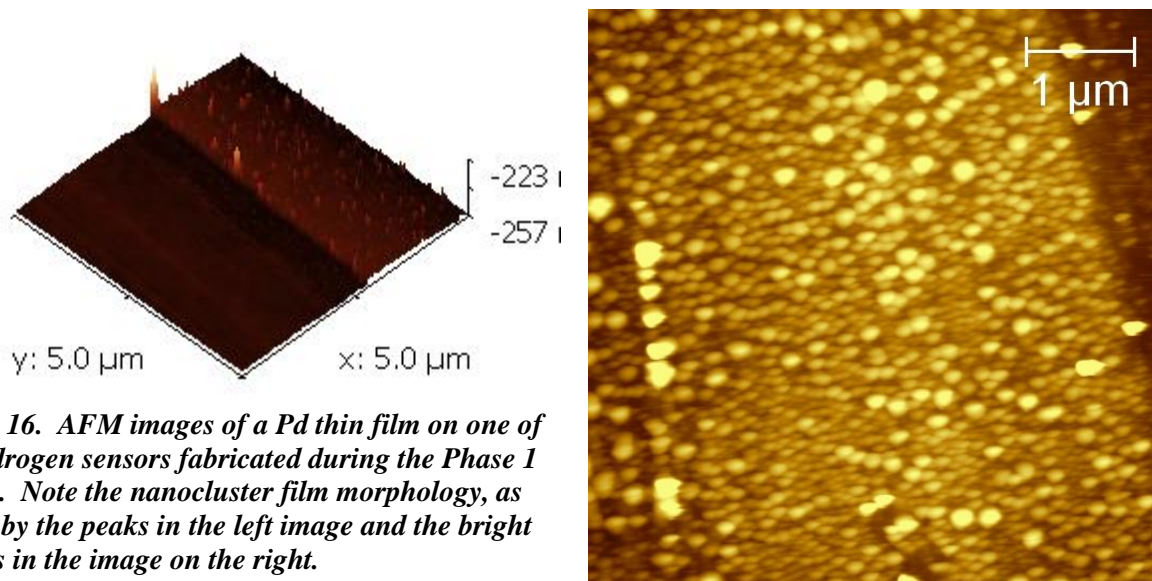


Figure 16. AFM images of a Pd thin film on one of the hydrogen sensors fabricated during the Phase I project. Note the nanocluster film morphology, as shown by the peaks in the left image and the bright regions in the image on the right.

Task 4.1.6 – Sensor Testing: The PSD hydrogen sensors were tested, and found to detect hydrogen at concentrations down to 1 ppm, as shown in Figure 17 below. The hydrogen sensors developed exhibited large initial responses to exposure to hydrogen gas, and we theorize this is due to a permanent morphology change that occurs in the Pd film upon exposure to hydrogen. Figure 18 shows a typical response upon initial exposure of one sample film. For this film, the device response before exposure was at -95 dB (still well above the noise floor of the network analyzer used for these measurements). Introduction of hydrogen at 8% caused a very rapid increase in signal level of 10 dB, followed by a slow additional increase in signal level of more than 12 dB. This process continued until the device response leveled off, a process that took several hours worth of gas exposure. This slow process represents an irreversible change in the sensor device response, and can either be taken advantage of to produce hydrogen leak alarm sensors that are single use, or can be treated as a device aging mechanism. With a long enough hydrogen exposure, the device response settles at a final level. When hydrogen is removed, the response drops slightly, and remains stable at level slightly below the level reached during aging. Upon subsequent exposure to hydrogen, the sensor responds with a rapid increase in signal level, approaching the level "fully aged" response level previously attained.

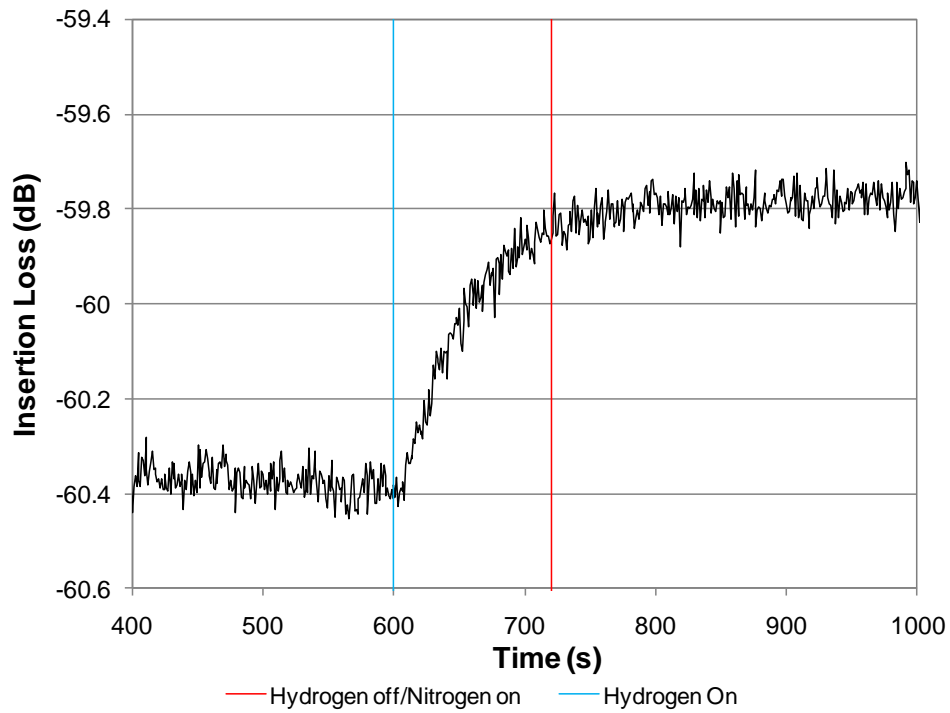


Figure 17. Hydrogen exposure at 1 ppm as detected by a SAW sensor during Phase I program. This response was not the initial response of this film to hydrogen, but was a response obtained upon repeated exposure.

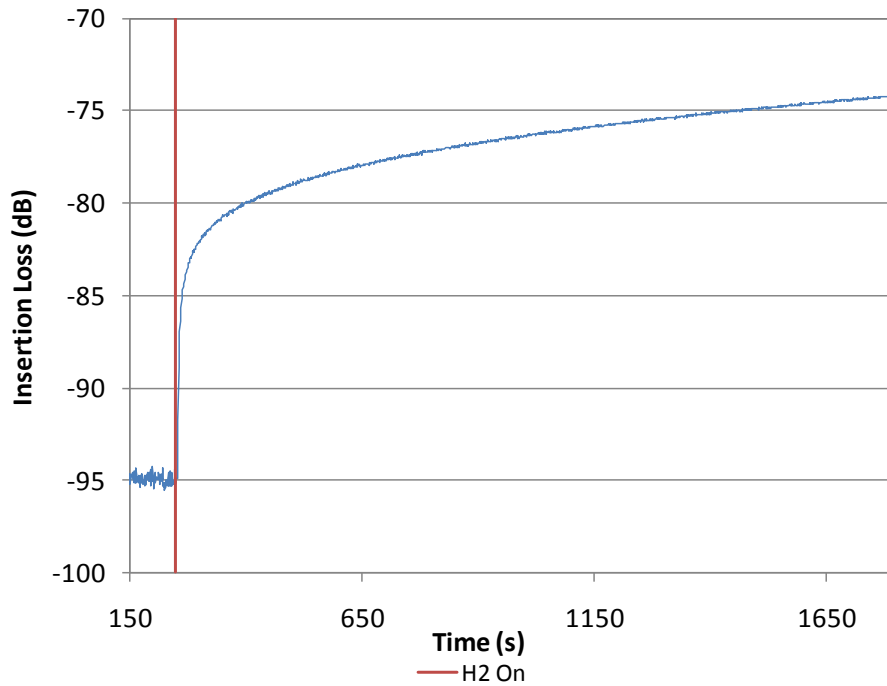


Figure 18. Response of a (QCM measured) 11Å Pd film to initial H₂ exposure at 8% with N₂ carrier gas.

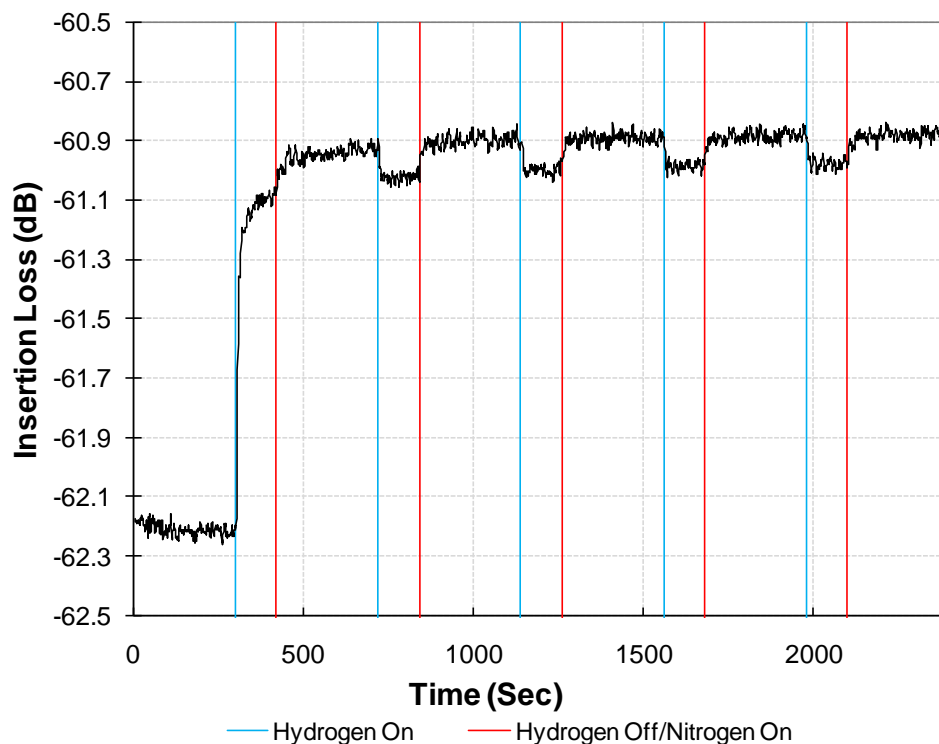


Figure 19. Response of SAW PSD hydrogen sensor with QCM-measured 13Å Pd films to 1000ppm H₂ cycling with N₂ carrier and purge gas.

Cycling between hydrogen and carrier gas exposure thereafter causes the device response to drop slightly when hydrogen is introduced, and return to the "fully aged" level when hydrogen is turned off and purge gas introduced. This effect is shown in Figure 19 above. Note the stable, repeatable responses to exposure of the fully aged device once the initial jump in response has occurred. This large initial reaction to hydrogen, which is much more rapid than that of a non-aged device, could be useful for alarm purposes, although it is not reversible until several minutes after the hydrogen exposure is stopped, and hence cannot be viewed as "reversible". Alternatively, the smaller reversible response produces predictable amplitude changes with the presence of hydrogen. These amplitude changes can (in theory) be used to precisely detect the concentration of hydrogen present as the change is proportional to the concentration of H₂. Pre-aging of devices would be required in practice if either the rapid initial response shown in Figure 19 or the reversible response was going to be used in applications, since these responses only become stable and repeatable after this aging process.

The mechanisms responsible for the relatively complex hydrogen responses exhibited by these sensors have not yet been determined. The large, irreversible increase in signal level upon first exposure, the sizeable and rapid initial increase in signal response upon subsequent initial exposure, and the later reduction in signal level upon repeated exposure are fascinating and will require additional

research to clarify the physical mechanisms responsible for the observed device performance.

Additional testing with films of different thicknesses, with hydrogen at concentrations ranging from 8% down to 1 ppm, with nitrogen and dry air as carrier gases produced mixed results.

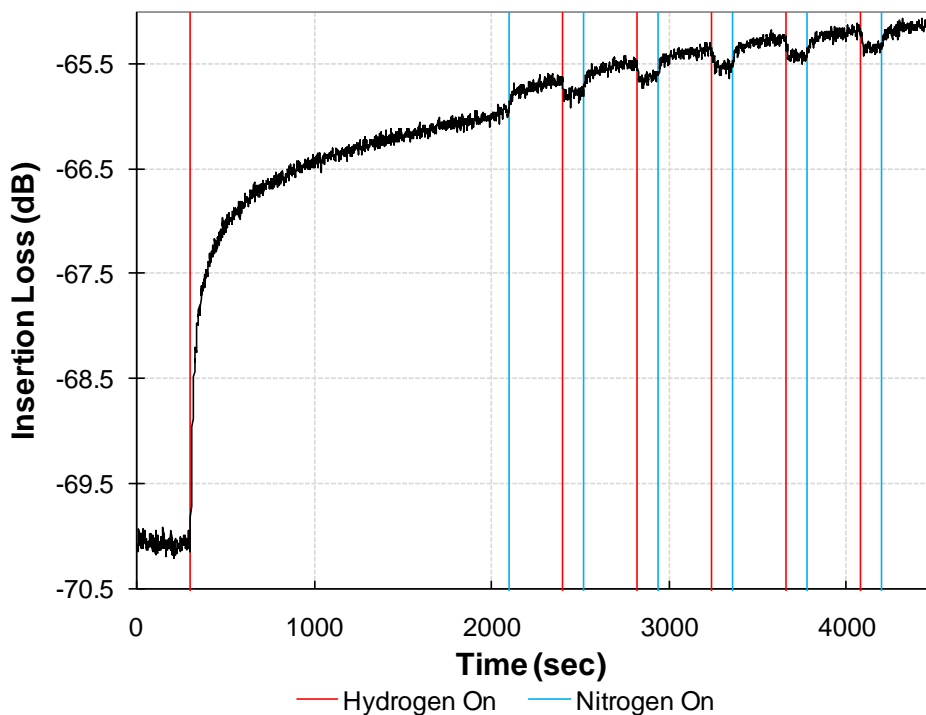


Figure 20. First Exposure PSD sensor with 13Å Pd(QCM) 1000ppm H₂ cycling with N₂ carrier.

Figure 20 graph shows the first exposure of a device with 13 Å of palladium (as measured by the QCM) to 1000ppm H₂ in nitrogen. As in the device of Figure 18, the large initial response is potentially useful as a single-use hydrogen leak detector, as this is an irreversible response. This film was subjected to hydrogen cycling tests prior to allowing the film to complete the initial exposure aging process. As the hydrogen is cycled on and off a consistent reversible reaction can be seen. Had this device been allowed to soak in hydrogen longer, these responses would appear level like those of the device in Figure 19, although they would also be twice as large in amplitude (0.2 dB vs. 0.1 dB).

When the device of Figure 19 (which has been well aged and is stable) is exposed to 100ppm H₂, the initial response is still quite large at about 0.6 dB (vs. 1 dB at 1000 ppm) as shown in Figure 21. This would be useful in a threshold alarm device. However, subsequent cycling of hydrogen at 100 ppm produces a response small enough that it can barely be discerned as a signal. This reversible response is not useful as the S/N is too low.

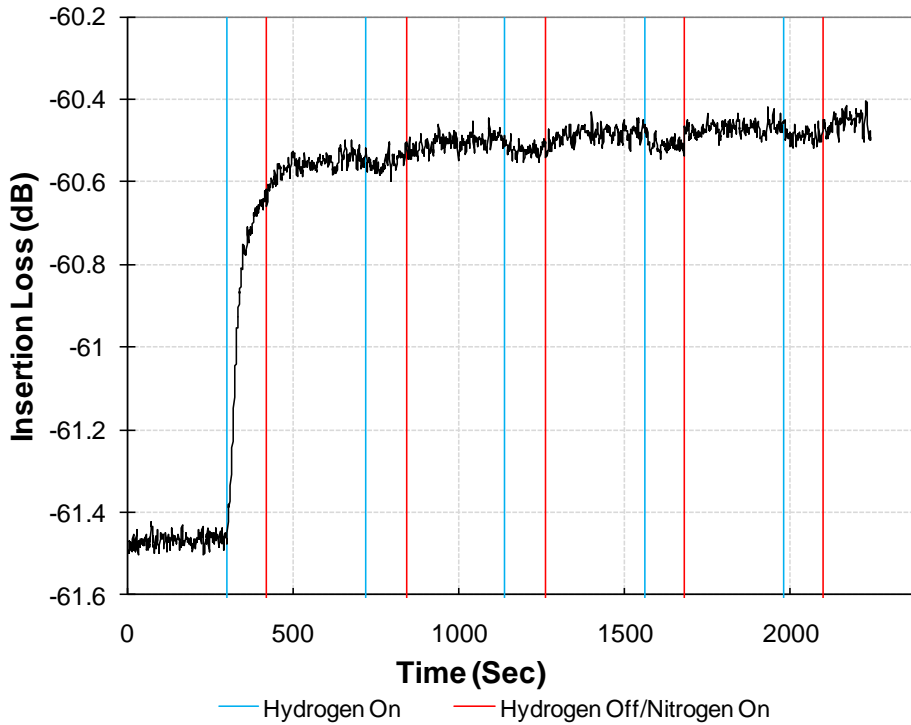


Figure 21. Response of SAW PSD hydrogen sensor with QCM-measured 13Å Pd films (the same device as shown in Figures 17 & 19) to 100ppm H₂ cycling with N₂ carrier & purge gas.

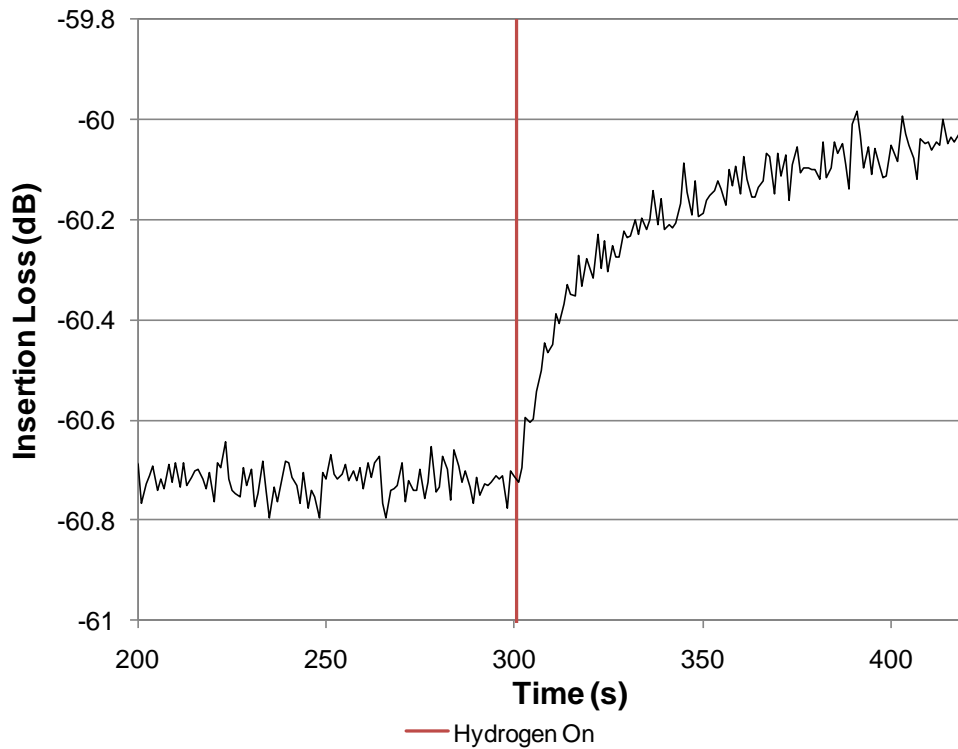


Figure 22. Response of the SAW PSD hydrogen sensor of Figures 17, 19 and 21 to 10ppm H₂ with N₂ carrier gas.

REPORT DOCUMENTATION PAGE

Form Approved
OMB No. 0704-0188

Public reporting burden for this collection of information is estimated to average 1 hour per response, including the time for reviewing instructions, searching existing data sources, gathering and maintaining the data needed, and completing and reviewing the collection of information. Send comments regarding this burden estimate or any other aspect of this collection of information, including suggestions for reducing this burden, to Department of Defense, Washington Headquarters Services, Directorate for Information Operations and Reports (0704-0188), 1215 Jefferson Davis Highway, Suite 1204, Arlington, VA 22202-4302. Respondents should be aware that notwithstanding any other provision of law, no person shall be subject to any penalty for failing to comply with a collection of information if it does not display a currently valid OMB control number.

PLEASE DO NOT RETURN YOUR FORM TO THE ABOVE ADDRESS.

1. REPORT DATE (DD-MM-YYYY) 29-07-2010		2. REPORT TYPE Final Report		3. DATES COVERED (From - To) Jan 29, 2010 – July 29, 2010	
4. TITLE AND SUBTITLE Rapid Hydrogen and Methane Sensors for Wireless Leak Detection				5a. CONTRACT NUMBER NNX10CD41P	
				5b. GRANT NUMBER	
				5c. PROGRAM ELEMENT NUMBER	
6. AUTHOR(S) Hines, Jacqueline H., PI Randles, Andrew B. Hines, Andrew T.				5d. PROJECT NUMBER	
				5e. TASK NUMBER	
				5f. WORK UNIT NUMBER	
7. PERFORMING ORGANIZATION NAME(S) AND ADDRESS(ES) Applied Sensor Research & Development Corporation 1195 Baltimore Annapolis Blvd, Unit #2, Arnold MD 21012				8. PERFORMING ORGANIZATION REPORT NUMBER ASRD R1016 FR	
9. SPONSORING/MONITORING AGENCY NAME(S) AND ADDRESS(ES) National Aeronautics and Space Administration NASA/ Shared Service Center, Bldg. 1111, C Road Stennis Space Center MS 39529-6000 COTR: Gary W. Hunter (GRC)				10. SPONSORING/MONITOR'S ACRONYM(S) NASA//GRC	
				11. SPONSORING/MONITORING REPORT NUMBER	
12. DISTRIBUTION/AVAILABILITY STATEMENT Pages 12-13 and 19-27 contain ASR&D proprietary information and are subject to the terms restricting release of proprietary information contained in the contract. The remainder of the report is available for unrestricted release.					
13. SUPPLEMENTARY NOTES					
14. ABSTRACT This report describes progress made during the this Phase 1 SBIR contract on the development of passive wireless surface acoustic wave (SAW) sensors for hydrogen and for methane. These sensors demonstrated real-time measurement of low levels of hydrogen (down to 1 ppm). Sensing of methane was less promising (measured at 1% methane in nitrogen), due to difficulties with cryptophane film deposition. Additionally, a real-time deposition monitor for thin conductive films was developed, and used to monitor e-beam deposition of ultrathin Pd films (from 2 to 50 angstroms thick).					
15. SUBJECT TERMS SAW (surface acoustic wave), sensor, passive, wireless, hydrogen, methane					
16. SECURITY CLASSIFICATION OF:			17. LIMITATION OF ABSTRACT UU	18. NUMBER OF PAGES 27 (plus this form)	19a. NAME OF RESPONSIBLE PERSON Jacqueline Hines
a. REPORT U	b. ABSTRACT U	c. THISPAGE U			19b. TELEPHONE NUMBER (Include area code) 410-544-4664